

## DIRECT TORQUE CONTROL OF MULTI-PHASE INDUCTION MOTOR WITH FUZZY LOGIC SPEED CONTROLLER

Jacek Listwan

Wrocław University of Science and Technology, Department of Electrical Machines, Drives and Measurements

**Abstract.** The paper presents the Direct Torque Control with Space Vector Modulation (DTC-SVM) of seven-phase induction motor with Fuzzy Logic Speed Controller. The mathematical model of the seven-phase squirrel-cage induction motor and chosen methods of Space Vector Modulation have been presented. Simulation studies of the DTC-SVM with Fuzzy Logic speed controller have been carried out and the results of simulation studies have been presented and discussed. The author original contribution includes analysis and studies of considered control method of seven-phase induction motor.

**Keywords:** seven-phase induction motor, Direct Torque Control, Space Vector Modulation, Fuzzy Logic Control

### BEZPOŚREDNIE STEROWANIE MOMENTEM WIELOFAZOWEGO SILNIKA INDUKCYJNEGO Z ROZMYTYM REGULATOREM PRĘDKOŚCI

**Streszczenie.** W artykule przedstawiono metodę bezpośredniego sterowania momentem siedmofazowego silnika indukcyjnego z zastosowaniem metod modulacji wektorowej i rozmytego regulatora prędkości. Przedstawiono model matematyczny siedmofazowego silnika indukcyjnego klatkowego oraz wybrane metody modulacji wektorowej. Przeprowadzono badania symulacyjne sterowania silnikiem z zastosowaniem metody DTC-SVM i rozmytego regulatora prędkości. Przedstawiono i omówiono wyniki badań symulacyjnych. Oryginalny wkład autora dotyczy analizy i badań przedstawionej metody sterowania silnikiem siedmofazowym.

**Słowa kluczowe:** silnik indukcyjny 7-fazowy, bezpośrednie sterowanie momentem, metody modulacji wektorowej, sterowanie rozmyte

### Introduction

Nowadays, the three-phase induction motors are predominately used in the variable speed electric drives. However, due to the development of the converter systems there is a great interest in the using of the constructions of induction motors with the number of the stator winding phases greater than three. The main advantages of these types of motors are lower torque pulsations, reduction of the stator current per phase and greater motor reliability. The multi-phase induction motors may be conditionally operated at failure of one or more stator phases [3, 5, 6, 8, 11]. In this paper the seven-phase squirrel-cage induction motor is considered. The seven-phase motors can be used in high power applications and in drive systems with specific requirements for accuracy of control and reliability [1, 3].

In this paper the novel system of Direct Torque Control of seven-phase squirrel-cage induction motor with Space Vector Modulation and Fuzzy Logic speed controller has been considered and described. The Fuzzy Logic controllers have the nonlinear control surfaces and can give much better control results in comparison with the conventional linear controllers [2, 4, 10]. The aim of the Direct Torque Control method with Space Vector Modulation (DTC-SVM) is the control of the motor angular speed, the magnitude of the stator flux vector and the motor electromagnetic torque [7].

This paper has been divided into eight sections. Section 1 provides an introduction. Section 2 is dedicated to the mathematical model of the seven-phase squirrel-cage induction motor. In the section 3 the mathematical model of the seven-phase Voltage Source Inverter (VSI) is presented. The Space Vector Modulation (SVM) methods have been discussed in the Section 4 and the applied Fuzzy Logic controller is presented in the Section 5. Section 6 is dedicated to the description of the DTC-SVM control system. The results of the conducted simulation studies have been presented in the Section 7. Section 8 concludes the paper.

### 1. Mathematical model of seven-phase squirrel-cage induction motor

Mathematical model of the seven-phase squirrel-cage induction motor has been formulated on the basis of commonly used simplifying assumptions presented in detail in [5, 8]. The

general scheme of the stator and rotor windings of the seven-phase squirrel-cage induction motor has been presented in Figure 1.

Mathematical model of seven-phase induction motor in phase coordinate systems is described by the set of differential equations with the coefficients changing as a function of angle rotation of the rotor [3, 5, 8]. The equations of seven-phase induction motor expressed through phase variables can be transformed to equations with constant coefficients by the use of the appropriate transformation of variables.

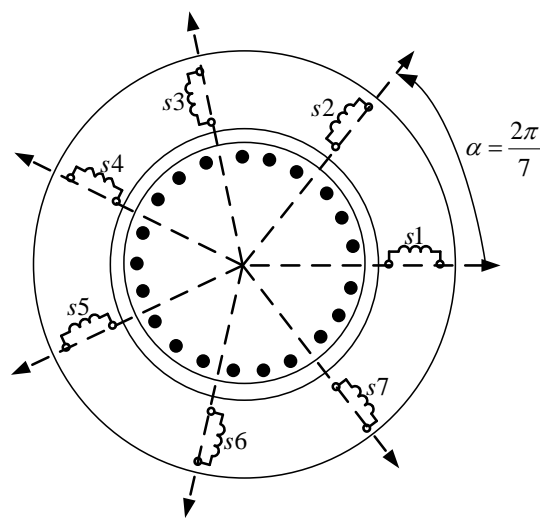


Fig. 1. General scheme of the stator and rotor windings of seven-phase squirrel-cage induction motor

The transformation of stator variables can be made by using the transformation matrixes denoted as  $[C]$  and  $[D_s]$  and the transformation of rotor variables can be made by using the transformation matrixes denoted as  $[C]$  and  $[D_r]$  [8].

After applying the transformation matrixes denoted as  $[C]$  to the stator and rotor equations, the original seven-phase system can be decomposed into decoupled systems: the stationary  $\alpha$ - $\beta$  coordinate system, the additional coordinate systems  $z_1$ - $z_2$  and  $z_3$ - $z_4$  and the system of zero components (there is one zero component for the considered induction motor).

The transformation matrix  $[C]$  for seven-phase induction motor is defined as follows [8]:

$$[C] = \frac{2}{7} \begin{bmatrix} \alpha & 1 & \cos \alpha & \cos 2\alpha & \cos 3\alpha & \cos 4\alpha & \cos 5\alpha & \cos 6\alpha \\ \beta & 0 & \sin \alpha & \sin 2\alpha & \sin 3\alpha & \sin 4\alpha & \sin 5\alpha & \sin 6\alpha \\ z_1 & 1 & \cos 2\alpha & \cos 4\alpha & \cos 6\alpha & \cos 8\alpha & \cos 10\alpha & \cos 12\alpha \\ z_2 & 0 & \sin 2\alpha & \sin 4\alpha & \sin 6\alpha & \sin 8\alpha & \sin 10\alpha & \sin 12\alpha \\ z_3 & 1 & \cos 3\alpha & \cos 6\alpha & \cos 9\alpha & \cos 12\alpha & \cos 15\alpha & \cos 18\alpha \\ z_4 & 0 & \sin 3\alpha & \sin 6\alpha & \sin 9\alpha & \sin 12\alpha & \sin 15\alpha & \sin 18\alpha \\ 0 & 1/\sqrt{2} & 1/\sqrt{2} & 1/\sqrt{2} & 1/\sqrt{2} & 1/\sqrt{2} & 1/\sqrt{2} & 1/\sqrt{2} \end{bmatrix} \quad (1)$$

where:  $\alpha = 2\pi/7$  – is the electrical angle between the axes of the machine phase windings.

The components in coordinate system  $\alpha$ - $\beta$  can be transformed to the general common  $x$ - $y$  coordinate system, which rotates at arbitrary angular speed  $\omega_k$  by using the  $[D]$  transformation matrix. The elements of the  $[D_s]$  and  $[D_r]$  transformation matrixes are defined as follows [8]:

$$[D_s] = [D_s(\vartheta_k)] = \begin{bmatrix} \cos \vartheta_k & \sin \vartheta_k \\ -\sin \vartheta_k & \cos \vartheta_k \end{bmatrix} \text{diag}[1]_{(n-2) \times (n-2)} \quad (2)$$

$$[D_r] = [D_r(\vartheta_k - \varphi_e)] = \begin{bmatrix} \cos(\vartheta_k - \varphi_e) & \sin(\vartheta_k - \varphi_e) \\ -\sin(\vartheta_k - \varphi_e) & \cos(\vartheta_k - \varphi_e) \end{bmatrix} \text{diag}[1]_{(n-2) \times (n-2)} \quad (3)$$

where:  $\vartheta_k = \int_0^t \omega_k dt$ ;  $\omega_k$  – the arbitrary angular speed of the coordinate system relative to the stator;  $n$  – the number of the stator phases (for the considered motor  $n = 7$ ).

The equations of seven-phase induction motor after transformations of variables have the following form [3, 5, 8]:

- the voltage equations of the stator and rotor in the  $x$ - $y$  coordinate system:

$$u_{sx} = R_s i_{sx} - \omega_k \psi_{sy} + p \psi_{sx} \quad (4)$$

$$u_{sy} = R_s i_{sy} + \omega_k \psi_{sx} + p \psi_{sy} \quad (5)$$

$$0 = R_r i_{rx} - (\omega_k - \omega_e) \psi_{ry} + p \psi_{rx} \quad (6)$$

$$0 = R_r i_{ry} + (\omega_k - \omega_e) \psi_{rx} + p \psi_{ry} \quad (7)$$

- the stator voltage equations in the additional coordinate systems  $z1$ - $z2$  and  $z3$ - $z4$ :

$$u_{sz1} = R_s i_{sz1} + p \psi_{sz1} \quad (8)$$

$$u_{sz2} = R_s i_{sz2} + p \psi_{sz2} \quad (9)$$

$$u_{sz3} = R_s i_{sz3} + p \psi_{sz3} \quad (10)$$

$$u_{sz4} = R_s i_{sz4} + p \psi_{sz4} \quad (11)$$

- the equation of the motor electromagnetic torque:

$$T_e = \frac{7}{2} p_b (\psi_{sy} i_{rx} - \psi_{sx} i_{ry}) \quad (12)$$

- mechanical motion equation:

$$T_e - T_m = \frac{J_m}{p_b} p \omega_e \quad (13)$$

where:  $u_{sx}$ ,  $u_{sy}$  – components of the stator voltage vectors in the  $x$ - $y$  coordinate system;  $u_{sz1}, \dots, u_{sz4}$  – components of the stator voltage vectors in the additional  $z1$ - $z2$  and  $z3$ - $z4$  coordinate systems;  $i_{sx}$ ,  $i_{sy}$ ,  $i_{rx}$ ,  $i_{ry}$  – components of the stator and rotor current vectors in the  $x$ - $y$  coordinate system;  $i_{sz1}, \dots, i_{sz4}$  – components of the stator current vector in the additional  $z1$ - $z2$  and  $z3$ - $z4$  coordinate systems;  $\psi_{sx}$ ,  $\psi_{sy}$ ,  $\psi_{rx}$ ,  $\psi_{ry}$  – components of the stator and rotor flux linkage vectors in the  $x$ - $y$  coordinate system;

$\psi_{sz1}, \dots, \psi_{sz4}$  – components of the stator flux linkage vectors in the additional  $z1$ - $z2$  and  $z3$ - $z4$  coordinate systems;  $\omega_e$  – the electrical angular speed of the motor;  $R_s$ ,  $R_r$  – stator and rotor phase resistance;  $p_b$  – the number of motor pole pairs;  $p = d/dt$  – derivative operator;  $T_e$  – the motor electromagnetic torque;  $T_m$  – the load torque;  $J_m$  – the inertia of the drive system.

The values of variables considered in the additional coordinate systems  $z1$ - $z2$  and  $z3$ - $z4$  are not involved in the generation of the motor electromagnetic torque. However they must be considered in the analysis and minimized with the use of the appropriate control structures, because they can cause enlargement of the amplitude of the stator phase currents and power losses in the stator windings [3, 5, 8].

The values of the rotor components in the additional  $z1$ - $z2$  and  $z3$ - $z4$  coordinate systems and the values of stator and rotor zero sequence components are equal to zero because the rotor is short-circuited and the star connection of stator phase windings is assumed. The equations for these components are neglected in the analysis.

## 2. Mathematical model of the seven-phase Voltage Source Inverter

The scheme of the two-level seven-phase VSI used for control of the seven-phase induction motor is shown in Figure 2.

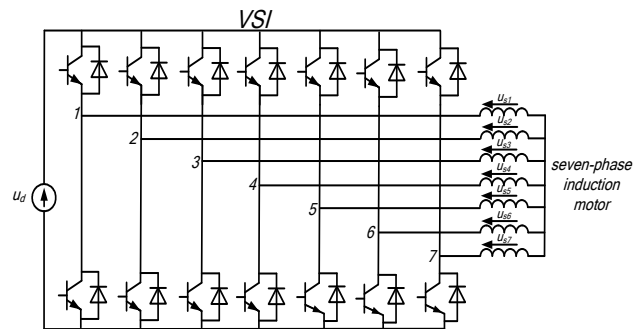


Fig. 2. Seven-phase induction motor supplied by the seven-phase VSI

Stator voltage space vectors generated by the seven-phase VSI in the stationary coordinate system  $\alpha$ - $\beta$  and additional coordinate systems  $z1$ - $z2$  and  $z3$ - $z4$  can be determined in general form [3]:

$$u_{s\alpha\beta} = u_{s\alpha} + j u_{s\beta} = \frac{2}{7} (S_1 + a S_2 + a^2 S_3 + a^3 S_4 + a^4 S_5 + a^5 S_6 + a^6 S_7) u_d \quad (14)$$

$$u_{sz1z2} = u_{sz1} + j u_{sz2} = \frac{2}{7} (S_1 + a^2 S_2 + a^4 S_3 + a^6 S_4 + a^8 S_5 + a^{10} S_6 + a^{12} S_7) u_d \quad (15)$$

$$u_{sz3z4} = u_{sz3} + j u_{sz4} = \frac{2}{7} (S_1 + a^3 S_2 + a^6 S_3 + a^9 S_4 + a^{12} S_5 + a^{15} S_6 + a^{18} S_7) u_d \quad (16)$$

where:  $a = \exp(j2\pi/7)$ ;  $S_1, \dots, S_7$  – the states of the switches of the seven-phase Voltage Source Inverter ( $S_i = 0$  or  $1$ ,  $i = 1, \dots, 7$ ).

The seven-phase VSI generates  $2^7 = 128$  output stator voltage space vectors. In the set of all generated voltage vectors, 126 active vectors and 2 zero vectors can be identified. The active space vectors have different magnitudes and divide the surface of voltage vectors into fourteen sectors [3].

Voltage space vectors generated by the seven-phase VSI in the coordinate system  $\alpha$ - $\beta$  are presented in Fig. 3a), voltage space vectors generated in the additional coordinate system  $z1$ - $z2$  are presented in the Fig. 3b) and in the additional coordinate system  $z3$ - $z4$  are presented in Fig. 3c).

All voltage space vectors presented in Fig. 3 have been identified with decimal numbers and these numbers can be converted into seven-position binary numbers. These binary numbers determine the states of the individual switches of the seven-phase VSI.

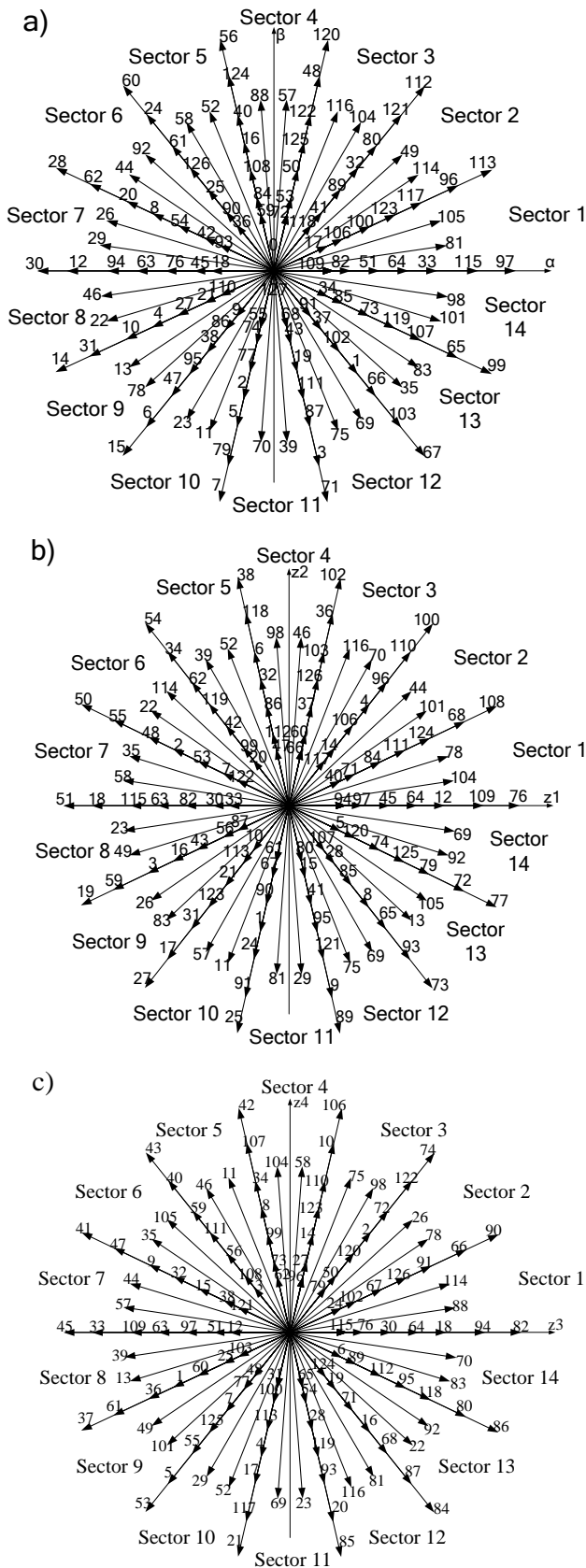


Fig. 3. Voltage space vectors generated by seven-phase VSI: a) in the stationary coordinate system  $\alpha$ - $\beta$ ; b) in the additional coordinate system  $z1$ - $z2$  c) in the additional coordinate system  $z3$ - $z4$

### 3. Space Vector modulation method

Due to a great number of voltage space vectors, the different concepts of Space Vector Modulation can be adopted for control of seven-phase Voltage Source Inverter [3]. In this article two concepts of the synthesis of the reference voltage vectors have been analyzed. In the first concept the switching times of two long voltage vectors chosen from the same sector in which the reference voltage vector is located and two zero voltage vectors have been applied. In the second concept the using of switching times of six active voltage vectors from the same sector and two zero voltage vectors have been chosen.

Graphical interpretation of the first concept of Space Vector Modulation method has been presented in Figure 4. The voltage space vectors in the  $\alpha$ - $\beta$  plane and the case when the reference voltage vector  $\underline{u}_{sref}$  is situated in Sector 1 are considered.

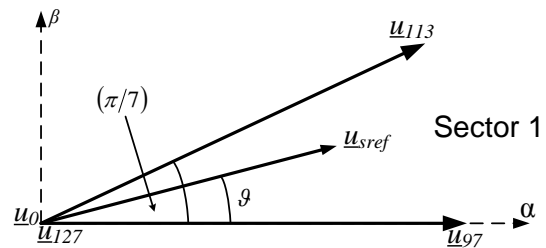


Fig. 4. The principle of determining the reference voltage vector with the choice of long voltage vectors

In this case the reference voltage vector is synthesized through using two long voltage vectors:  $\underline{u}_{97}$ ,  $\underline{u}_{113}$  and two zero voltage vectors:  $\underline{u}_0$ ,  $\underline{u}_{127}$ . The principle of Space Vector Modulation method can be described by the following general equations:

$$\underline{u}_{sref} \cdot T_s = \underline{u}_{97} \cdot t_{a1} + \underline{u}_{113} \cdot t_{b1} \quad (17)$$

$$t_0 = T_s - (t_{a1} + t_{b1}) \quad (18)$$

where:  $t_{a1}$ ,  $t_{b1}$  – switching times of long active voltage vectors;  $t_0$  – switching time of zero voltage vectors;  $\underline{u}_{sref}$  – magnitude of the reference voltage vector;  $T_s$  – switching period.

Graphical interpretation of the second concept of Space Vector Modulation method has been presented in Figure 5. The voltage space vectors in the  $\alpha$ - $\beta$  plane and the case when the reference voltage vector  $\underline{u}_{sref}$  is situated in Sector 1 are considered.

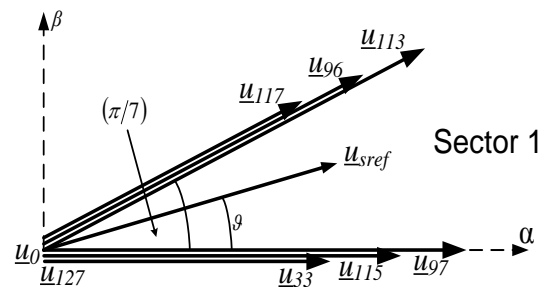


Fig. 5. The principle of determining the reference voltage vector with the choice of six active voltage vectors

In this case the reference voltage vector is synthesized by using six active voltage vectors:  $\underline{u}_{33}$ ,  $\underline{u}_{115}$ ,  $\underline{u}_{97}$ ,  $\underline{u}_{117}$ ,  $\underline{u}_{96}$ ,  $\underline{u}_{113}$  and two zero voltage vectors:  $\underline{u}_0$ ,  $\underline{u}_{127}$ . This concept of Space Vector Modulation allows to achieve the reference voltage vector in the  $\alpha$ - $\beta$  plane and at the same time to achieve the zero values of vectors in the additional  $z1$ - $z2$  and  $z3$ - $z4$  planes [3].

The principles of Space Vector Modulation method can be described by the following general equations:

$$\underline{u}_{sref} \cdot T_s = \underline{u}_{97} \cdot t_{a1} + \underline{u}_{113} \cdot t_{b1} + \underline{u}_{115} \cdot t_{a2} + \underline{u}_{96} \cdot t_{b2} + \underline{u}_{33} \cdot t_{a3} + \underline{u}_{117} \cdot t_{b3} \quad (19)$$

$$0 = \underline{u}_{76} \cdot t_{a1} + \underline{u}_{108} \cdot t_{b1} + \underline{u}_{109} \cdot t_{a2} + \underline{u}_{68} \cdot t_{b2} + \underline{u}_{12} \cdot t_{a3} + \underline{u}_{124} \cdot t_{b3} \quad (20)$$

$$0 = \underline{u}_{82} \cdot t_{a1} + \underline{u}_{90} \cdot t_{b1} + \underline{u}_{94} \cdot t_{a2} + \underline{u}_{66} \cdot t_{b2} + \underline{u}_{18} \cdot t_{a3} + \underline{u}_{91} \cdot t_{b3} \quad (21)$$

$$t_0 = T_s - (t_{a1} + t_{b1} + t_{a2} + t_{b2} + t_{a3} + t_{b3}) \quad (22)$$

where:  $t_{a2}$ ,  $t_{b2}$ ,  $t_{a3}$ ,  $t_{b3}$  – switching times of active voltage vectors.

Switching times of voltage vectors are calculated according to the equations (these formulas allow to ensure the average value of voltage in  $z1$ - $z2$  and in  $z3$ - $z4$  coordinate systems equal to zero) [3]:

$$t_{a1} = \sin(3\pi/7) \cdot \sin(s \cdot \pi/7 - \vartheta) \cdot \frac{u_{sref}}{u_d} \cdot T_s \quad (23)$$

$$t_{a2} = \sin(2\pi/7) \cdot \sin(s \cdot \pi/7 - \vartheta) \cdot \frac{u_{sref}}{u_d} \cdot T_s \quad (24)$$

$$t_{a3} = \sin(\pi/7) \cdot \sin(s \cdot \pi/7 - \vartheta) \cdot \frac{u_{sref}}{u_d} \cdot T_s \quad (25)$$

$$t_{b1} = \sin(3\pi/7) \cdot \sin[\vartheta - (s-1) \cdot \pi/7] \cdot \frac{u_{sref}}{u_d} \cdot T_s \quad (26)$$

$$t_{b2} = \sin(2\pi/7) \cdot \sin[\vartheta - (s-1) \cdot \pi/7] \cdot \frac{u_{sref}}{u_d} \cdot T_s \quad (27)$$

$$t_{b3} = \sin(\pi/7) \cdot \sin[\vartheta - (s-1) \cdot \pi/7] \cdot \frac{u_{sref}}{u_d} \cdot T_s \quad (28)$$

$$t_0 = T_s - (t_{a1} + t_{b1} + t_{a2} + t_{b2} + t_{a3} + t_{b3}) \quad (29)$$

where:  $\vartheta$  – the angle position of reference voltage vector,  $s$  – the number of sector.

#### 4. Fuzzy Logic controller

In the analyzed DTC-SVM control system the Fuzzy Logic speed controller has been applied. The block diagram of the selected Fuzzy Logic Controller (FLC) has been presented in Figure 6.

The applied FLC consists of five parts [2, 4, 10]:

- Part 1 is responsible for calculation of two control signals. The difference between the reference and calculated motor speed  $e$  is the first control signal. The time derivative of the first input signal  $\Delta e$  is the second control signal. The calculation of the output signals is performed with the use of the scaling factors  $k_e$  and  $k_{de}$ .
- The output signals from Part 1 are fuzzified in the Part 2. The triangle-shaped membership functions presented in Figure 7 have been used in this part of FLC.
- In Part 3 of the FLC the multiplication of the appropriate output signals from Part 2 is carried out.
- Part 4 is responsible for multiplication of the activation levels of the rules and weight coefficients. The weight coefficients were chosen as: N (negative), ZE (zero), P (positive), NB (negative big), NS (negative small), PS (positive small), PB (positive big).
- Part 5 is responsible for calculation of the output signal from FLC. The determination of the output signal is performed with the use of the scaling factor  $k_{du}$ . The output signal is calculated according to the following equation:

$$u(k) = \sum_{i=1}^n w_i a_i / \sum_{i=1}^n a_i \quad (30)$$

The scaling factors  $k_e$ ,  $k_{de}$  and  $k_{du}$  of the Fuzzy Logic controller have been matched with the use of genetic algorithm. The quality index K:

$$K = \min \left[ \int_0^{\infty} (\omega_e^* - \omega_e)^2 dt + \int_0^{\infty} (T_e^* - T_e)^2 dt + \int_0^{\infty} (\psi_s^* - \psi_s)^2 dt \right] \quad (31)$$

with the use of integral square error (ISE) criterion has been used in the FLC tuning procedure [10].

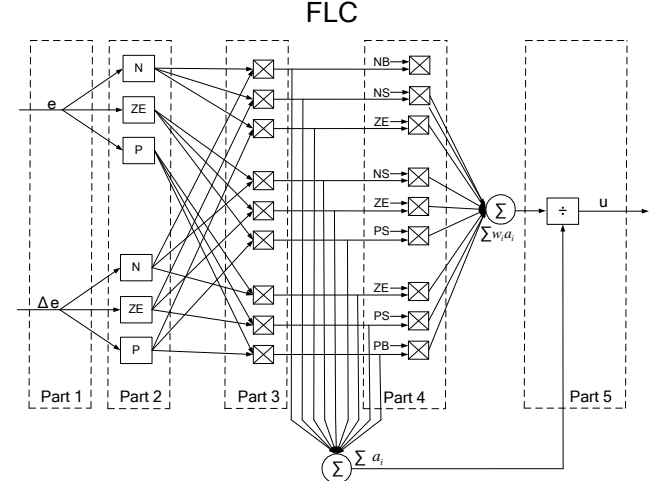


Fig. 6. The block diagram of the Fuzzy Logic speed controller

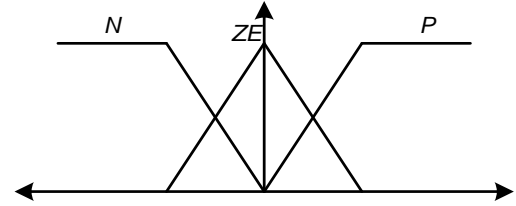


Fig. 7. The triangle-shaped membership function

#### 5. DTC-SVM control system

The block diagram of DTC-SVM control scheme of seven-phase induction motor is shown in Figure 8.

To implement the DTC-SVM control system the estimation block has been used [9]. The estimation block determines the instantaneous magnitude of the stator flux vector  $\psi_s$ , the estimated value of the motor electromagnetic torque  $T_e$  and the instantaneous angle  $\gamma_\psi$  of the stator flux vector position.

In the DTC-SVM control structure three control loops are applied: the control loop of motor angular speed  $\omega_e$  with Fuzzy Logic controller, the control loop of the motor electromagnetic torque  $T_e$  with PI controller and the control loop of the magnitude of the stator flux vector  $\psi_s$  with PI controller. Output signal from Fuzzy Logic controller of motor angular speed is the reference value of motor electromagnetic torque  $T_e^*$ . Output signal from electromagnetic torque controller is the reference value of the y component of the stator voltage vector  $u_{sy}^*$ . Output signal from controller of the magnitude of the stator flux vector is the reference value of the x component of the stator voltage vector  $u_{sx}^*$ . The reference values of components of the stator voltage vectors in the  $x$ - $y$  coordinate system are transformed to the  $\alpha$ - $\beta$  coordinate system and afterwards given to the Space Vector Modulation (SVM) block. The SVM sets the switching states of the seven-phase Voltage Source Inverter.

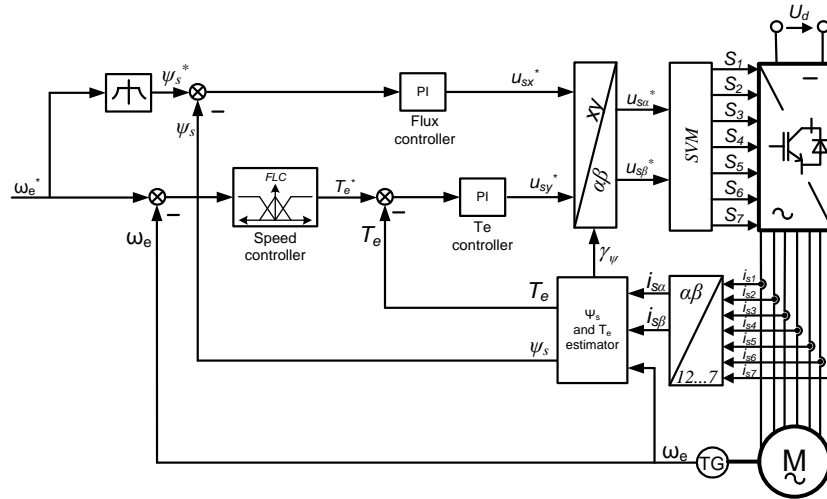


Fig. 8. DTC-SVM control system of seven-phase induction motor

### 6. Simulation results

Simulation studies were carried out for the seven-phase squirrel-cage induction motor with the following data:  $f_N = 50$  Hz,  $p_b = 2$ ,  $R_s = 10\Omega$ ,  $R_r = 6.3\Omega$ ,  $L_{ls} = L_{lr} = 0.04$  H,  $L_m = 0.42$  H. The simulation model of DTC-SVM control of seven-phase induction motor with Fuzzy Logic speed controller has been implemented in Matlab/Simulink® Software. The simulation studies of the considered control method were performed for the assumed trajectories of the reference motor speed and for variable values of the load torque. The second concept of the Space Vector Modulation method with the use of the six active voltage vectors and two zero voltage vectors has been applied in the simulation model.

The waveforms of the reference speed and calculated speed of the seven-phase induction motor have been presented in Figure 9. Analysis of this waveforms leads to the conclusion that the

calculated speed is with high accuracy equal to the reference speed.

The waveforms of the electromagnetic torque of the seven-phase induction motor and the load torque are presented in the Figure 10. The values of the electromagnetic torque depends on the reference trajectory of motor speed and values of the load torque.

Figure 12 shows the trajectory of the estimated values of the magnitude of the stator flux vector. It can be stated, that the magnitude of the stator flux vector is regulated at the nominal value.

The waveform of the stator phase current has been presented in Figure 11. It can be concluded, that the amplitudes of the stator phase current depend on the load condition of the drive system.

The waveforms of the stator current vector components in the  $z1$ - $z2$  coordinate system are shown in Figure 13. As a result of the applied Space Vector Modulation method, these components and components in the  $z3$ - $z4$  coordinate system have small amplitudes.

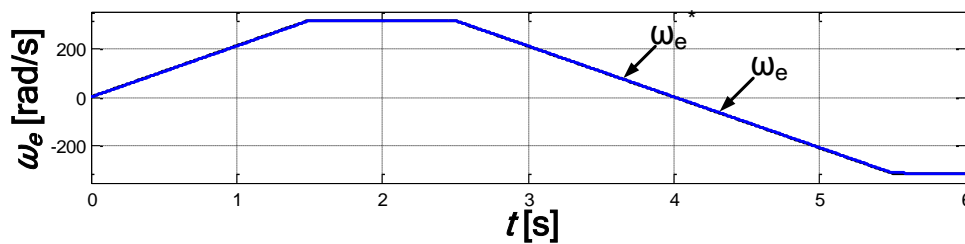


Fig. 9. The waveforms of reference and measured speeds of seven-phase induction motor for DTC-SVM with FLC

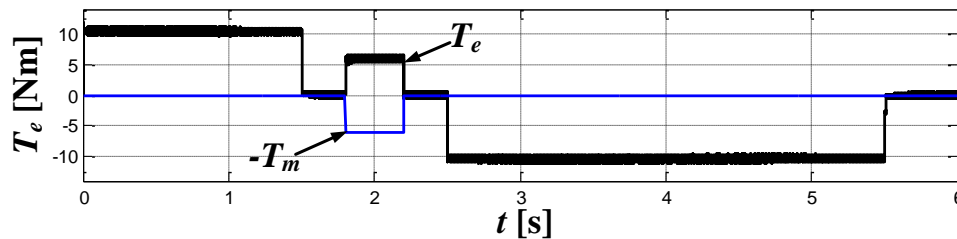


Fig. 10. The waveforms of the electromagnetic torque of seven-phase induction motor and the load torque for DTC-SVM with FLC

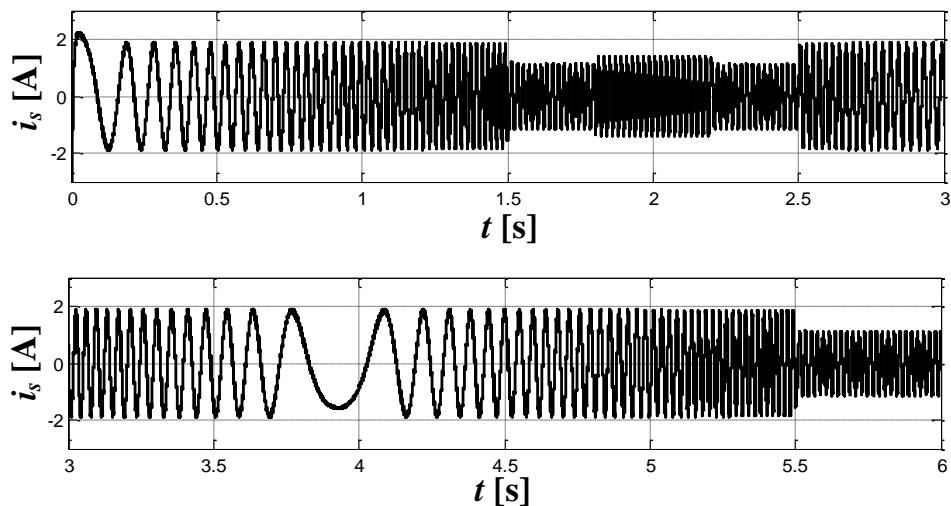


Fig. 11. The waveforms of the stator phase current of the seven-phase induction motor for DTC-SVM with FLC

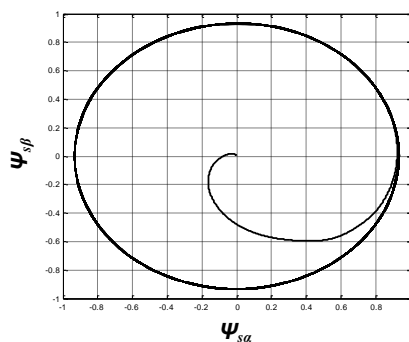


Fig. 12. Trajectory of the estimated magnitude of the stator flux vector

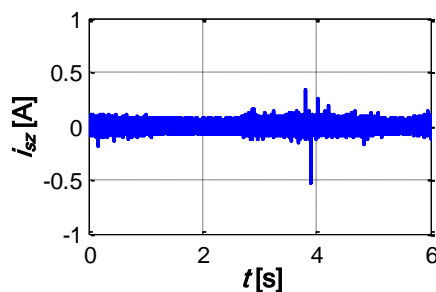


Fig. 13. The waveforms of the stator phase current vector components in the  $\alpha$ - $\beta$  additional coordinate system

## 7. Conclusions

The mathematical models of the seven-phase squirrel-cage induction motor and seven-phase Voltage Source Inverter have been presented. The chosen concepts of the Space Vector Modulation methods have been described, the scheme and description of the Fuzzy Logic Speed controller have been presented.

The structure of Direct Torque Control method with Space Vector Modulation with seven-phase induction motor and Fuzzy Logic speed controller has been presented and described.

Simulation studies of the considered control method were carried out and the results of the simulation studies have been presented and discussed. The analyzed control method allows for control of the given waveforms with great accuracy. The calculated motor speed is with high accuracy equal to the reference speed. The DTC-SVM system with Fuzzy Logic speed controller provides accurate control of the motor electromagnetic torque and the magnitude of the stator flux vector.

The drive system with Direct Torque Control of seven-phase induction motor and Fuzzy Logic speed controller can be used in industrial applications that require precise adjustment and reliable operation.

## References

- [1] Casadei D., Mengoni M., Serra G., Tani A., Zarri L., Parsa L.: Control of a High Torque Density Seven-Phase Induction Motor with Field-Weakening Capability. IEEE International Symposium on Industrial Electronics 2010, 2147–2152.
- [2] Derugo P., Szabat K.: Adaptive neuro-fuzzy PID controller for nonlinear drive system. COMPEL: The International Journal of Computation and Mathematics in Electrical and Electronic Engineering 34(3)/2015, 792–807.
- [3] Dujic D., Jones M., Levi E.: Generalised space vector PWM for sinusoidal output voltage generation with multiphase voltage source inverters. Int. J. Industrial Electronics and Drives 1(1)/2009, 1–13.
- [4] El-Barbary Z.M.S.: Fuzzy logic based controller for five-phase induction motor drive system. Alexandria Engineering Journal 51/2012, 263–268.
- [5] Levi E., Bojoi R., Profumo F., Toliyat H.A., Williamson S.: Multiphase induction motor drives - a technology status review. IET Electr. Power Appl., 2007, 489–516.
- [6] Listwan J., Pienkowski K.: Analysis of Vector Control of Multi-Phase Induction Motor. Prace Naukowe Instytutu Maszyn, Napędów i Pomiarów Elektrycznych Politechniki Wrocławskiej 65/2011, 305–319.
- [7] Lu S., Corzine K.: Direct torque control of five-phase induction motor using space vector modulation with harmonics elimination and optimal switching sequence. Applied Power Electronics Conference and Exposition, Dallas, 2006, 195–201.
- [8] Pienkowski K.: Analysis and Control of Multi-Phase Squirrel-Cage Induction Motor. Prace Naukowe Instytutu Maszyn, Napędów i Pomiarów Elektrycznych Politechniki Wrocławskiej 65/2011, 305–319.
- [9] Orłowska-Kowalska T.: Sensorless Induction Motor Drive. Wrocław University of Technology Press, Wrocław 2003.
- [10] Orłowska-Kowalska T., Szabat K.: Optimization of Fuzzy-Logic Speed Controller for DC Drive System With Elastic Joints. IEEE Transaction on Industry Applications 40(4)/2004, 1138–1144.
- [11] Zhao Y., Lipo T.A.: Space vector PWM Control of Dual Three-Phase Induction Machine Using Vector Space Decomposition. IEEE Transaction on Industry Applications 31(5)/1995, 1100–1109.

M.Sc. Jacek Listwan  
e-mail: jacek.listwan@pwr.edu.pl

Jacek Listwan received the M.Sc. degree in Control Engineering and Robotics from Faculty of Electrical Engineering, Wrocław University of Technology, Wrocław, Poland in 2013. He is a Ph.D. student in the Department of Electrical Machines, Drives and Measurements at the Wrocław University of Technology. His research interests include nonlinear control structures (Fuzzy Logic and Sliding-Mode) for multi-phase induction motors.



otrzymano/received: 15.06.2016

przyjęto do druku/accepted: 22.11.2017